AMERICAN JOURNAL OF BIOMEDICINE AND PHARMACY
https://biojournals.us/index.php/AJBP
ISSN: 2997-7177

Article

Dose-Dependent Reprogramming of Quorum Sensing and Biofilm-Matrix Transcripts During Ceftazidime Exposure and Washout in Pseudomonas aeruginosa: A Ten-Gene RT-qPCR Study

Hind Tahseen Ibrahim[1]

1. Medical physics department, collage of Science, Alfarahidi university, Baghdad, Iraq

Abstract: Background: Antibiotic exposure affects Las, Rhl, PQS and polysaccharide synthesis transcriptional programs in P. aeruginosa. Objective: To assess differences in transcriptional recovery post-exposure to weak and strong challenges of ceftazidime using an isolate-matched 10-gene panel. Methods: Twelve isolate-specific matched profiles were evaluated against CTRL, CAZ025 (0.25x MIC), CAZ050 (0.50x MIC) and WASH24 (24 hours drug-free after CAZ050). Short amplicon assays for ten genes were normalized to the geometric mean of proC and rpoD. Contrasts, Friedman tests, Wilcoxon sensitivity tests, and false discovery rate (FDR) analysis were performed. Principal component analysis (PCA) was also performed. Results: Out of the 10 comparisons between CAZ050 and CTRL, 10 met $q < 0.05$. The largest absolute change was observed for lasR at -0.97 $\log_2$ units (95% CI: -1.15, -0.80; $q < 0.0001$). Conclusions: Transcripts associated with QS, matrix and toxin synthesis, and motility provide a more comprehensive picture compared to that provided by a single QS transcript.

Keywords: Pseudomonas aeruginosa; ceftazidime; quorum sensing; biofilm; transcription; proC; rpoD; RT-qPCR.

Citation: Ibrahim H. T. Dose-Dependent Reprogramming of Quorum Sensing and Biofilm-Matrix Transcripts During Ceftazidime Exposure and Washout in Pseudomonas aeruginosa: A Ten-Gene RT-qPCR Study. American Journal of Biomedicine and Pharmacy. 2026, 3(11), 157-169.

Received: 10th Aug 2026
Revised: 11th Sep 2026
Accepted: 20th Oct 2026
Published: 25th Nov 2026

Copyright: © 2026 by the authors. Submitted for open access publication under the terms and conditions of the Creative Commons Attribution (CC BY) license (https://creativecommons.org/licenses/by/4.0/)

Introduction

Pseudomonas aeruginosa forms biofilms containing extracellular polymeric matrix which, along with phenotypic heterogeneity, complicates antibiotic exposure. [1] Quorum sensing is regulation of population density by which different bacterial communities produce and synthesize virulence factors. [2] There is cross talk among Las, Rhl and PQS circuits that cannot be explained by a single receptor transcript. [3] As one approach to modify quorum sensing within bacteria, investigation of antagonistic quorum sensing interactions is in progress. [4] Various molecular architectures of quorum sensing make it rational to assess multiple genes, instead of one. [5] Inconsistent assignments

of signaling molecules to circuits emphasize the need to precisely define the circuits being measured. [6] Natural antivirulence studies demonstrate that, within the same system, quorum sensing transcriptional regulation and surface-associated phenotypes may vary. [7] There are multiple possible mechanisms of action for silver-based compounds on microorganisms. [8] Nanoparticle exposure may result in the up-regulation of quorum sensing genes in some strains. [9] Exposure to sub-inhibitory concentrations of nanoparticles may not result in attenuation of virulence. [10] In a recent study of a mucoid isolate, the combination of ceftazidime and dihydroquercetin reduced more quorum-sensing and matrix-related transcripts as compared to each antibiotic alone. [11] Quorum Sensing is inhibited by antibiotic exposure and should be considered when interpreting transcriptional regulation studies. [12] Variations in the genetic background of strains may affect the outcome of regulatory studies.

Phenazine-associated toxicity is another endpoint unrelated to transcript abundance of the receptors. Receptor expression levels are altered during exposure to antibiotics and during quorum-sensing. Adaptive changes occurring during the washout period may explain some of these findings. Study design. The primary comparison was between CAZ050 and CTRL. The 0.25× CAZ and 24-hour washout conditions were the secondary comparisons. The goal of this study was to investigate whether the effects of CAZ on transcription showed a dose-dependent response and if matrix-bound genes involved in quorum-sensing also showed similar behavior.

Materials and methods

Quantitative study design

The study was designed to investigate effects of the four conditions, in 12 P. aeruginosa isolates, using control, CAZ at 0.25x MIC, CAZ at 0.50x MIC, and 24 hour post 0.50x MIC washout conditions. The matching factor was isolate ID, and the unit of interest for analysis was the isolate, not the reaction well.

Table 1. Study design, contrasts and independent statistical units

Arm	Condition	Independent units	Primary interpretation
CTRL	No ceftazidime	12 paired isolates	Isolate-specific baseline
CAZ025	0.25 × isolate MIC	12 paired isolates	Lower exposure response
CAZ050	0.50 × isolate MIC	12 paired isolates	Primary exposure contrast
WASH24	24 h drug-free after CAZ050	12 paired isolates	Post-exposure state

The sample profile unit was used in all statistical analyses; technical reaction replicates were aggregated before inference.

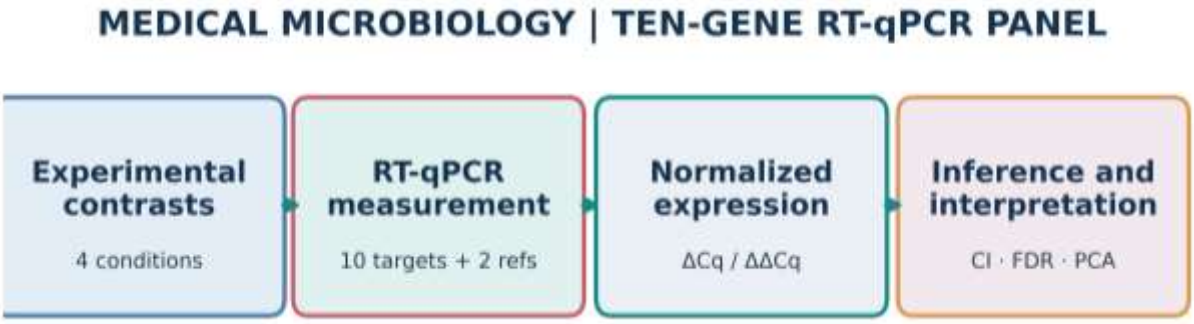

Figure 1. Study structure from independent-unit contrasts through primer verification, two-gene reference normalization, multiple-testing control and multivariate interpretation.

Molecular panel and published primer provenance

Regulatory transcripts comprised lasI, lasR, rhlI, rhlR, pqsA and mvfR (pqsR); downstream functional programs comprised fliC, pslA, pelA and toxA. References normalization was performed for proC and rpoD post across-condition Cq and interreference difference assessment. As reported in

the 2026 reference-gene study, stability of bacterial references is dependent on the growth medium, sampling time and bacterial genotype.

Table 2. Published RT-qPCR primer sequences for the ten target genes (5′→3′)

Target	Forward (5′→3′)	Reverse (5′→3′)	bp	Source
lasI	GTAGGCGTGGAGAAGATGATG	ATCTGGGTCTTGGCATTGAG	122	D-2022
lasR	CTGTGGATGCTCAAGGACTAC	CCACTGCAACACTTCCTTCT	111	D-2022
rhlI	GTCGGTCTGGGAGCTTTC	CAGGTACCAGGCGCATT	100	D-2022
rhlR	CTGTGGTGGGACGGTTTG	GGGTGAAGGGAATCGTGTG	139	D-2022
pqsA	GCTGTATTCGATTCCCAAGATG	CCAGGTATCGTCGAGCAG	100	D-2022
mvfR	GCTTCGCCTGATCCCTTAC	GCAGCACCCGGAGATTG	104	D-2022
fliC	CGACAAGGGTGTACTGACCA	GACCTTCACTGCGACCTGAC	100	E-2026
pslA	CGGTCAGCGAATACAGCTC	TTGATCTTGTGCAGGGTGTC	103	E-2026
pelA	GGAACAGCCAGGTAATGGAC	TCCAGGGTATCGAGGAACAG	112	E-2026
toxA	CCGCCGAAGACGATGCTT	CACCGCCAACTGGAGGAG	85	F-2021

bp = length reported in the cited publication; all products are ≤150 bp. Gene identifiers and source codes are defined in Table 4.

Table 3. Dual normalization primers and amplicon characteristics

Reference	Forward (5′→3′)	Reverse (5′→3′)	bp	Source
proC	GAGATCCAACTGATCGTCTCC	GGGTGTTGGGCATGCAG	100	D-2022
rpoD	CGAACTGCTTGCCGACTT	GCGAGAGCCTCAAGGATAC	131	F-2021

Two reference-gene Cq values were combined by arithmetic mean, equivalent to the geometric mean of reference abundances when amplification efficiencies are comparable.

Table 4. Assay targets, biological categories and primer-document source map

Gene	Functional scope	Panel	Published source
lasI	Las AHL synthase	QS	D-2022
lasR	Las transcriptional receptor	QS	D-2022
rhlI	Rhl AHL synthase	QS	D-2022
rhlR	Rhl transcriptional receptor	QS	D-2022
pqsA	PQS precursor biosynthesis	QS	D-2022
mvfR	PQS network regulator	QS	D-2022
fliC	Flagellar structural transcript	Biofilm/virulence	E-2026
pslA	Psl polysaccharide locus	Biofilm/virulence	E-2026
pelA	Pel polysaccharide locus	Biofilm/virulence	E-2026
toxA	Exotoxin A transcript	Biofilm/virulence	F-2021

Primer references: D-2022: Nishio et al., Microorganisms 2022, 10:1755; E-2026: Gao et al., Front Microbiol 2026, 17:1945324; F-2021: Inhibition of quorum sensing and virulence factors by gold and selenium nanoparticles, Antibiotics 2021, 10:1461.

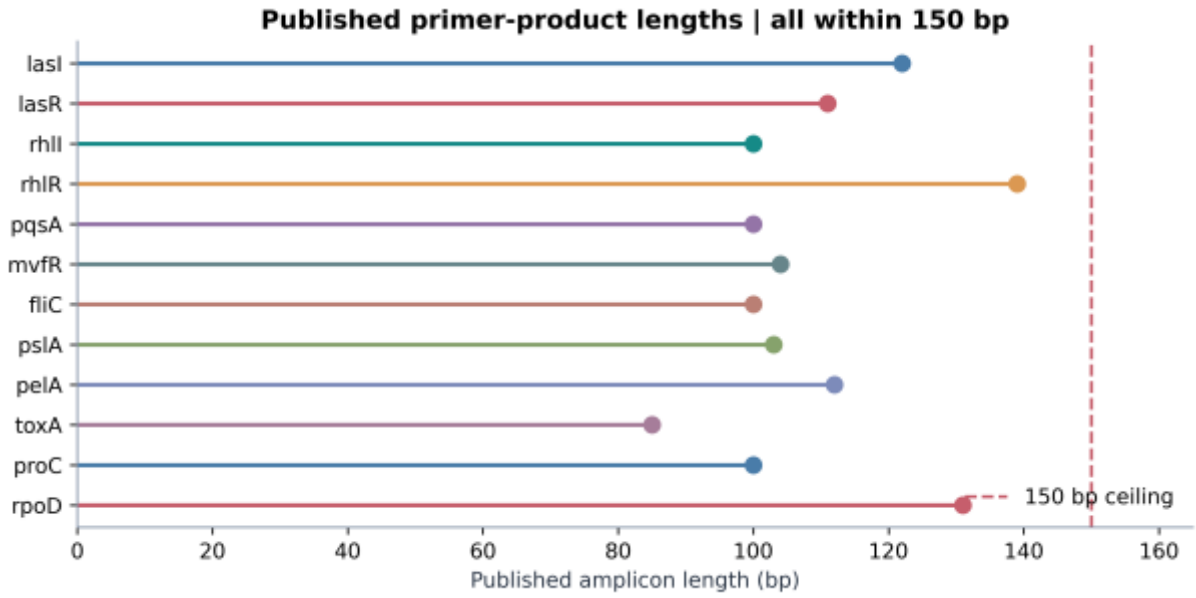

Figure 2. Short-amplicon product-size map for all ten target assays and both reference assays; the dashed line marks the prespecified 150-bp limit.

RNA workflow, assay controls and Cq generation

Total RNA isolated using the matched-pair bacterial method was processed with DNase treatment, equal-mass reverse transcription and quantitative real-time PCR using a 10 µL SYBR Green system. PCR conditions were 95°C for 2 min followed by 40 cycles of 95°C for 10s and 60°C for 30s. Melting curve analysis was performed post PCR. Reagent and no reverse transcriptase controls were included in each real-time PCR assay. Relative to each isolate's MIC, antibiotic concentrations were expressed. This was to avoid assigning the same absolute antibiotic concentration to all the isolates.

Reaction Cqs were averaged to obtain one value per biologic sample, prior to calculating the ΔCq. ΔCq = Cq (target) - ½ (Cq (reference 1) + Cq (reference 2)). ΔΔCq = ΔCq (sample) - mean ΔCq (control). Log_2 relative abundance = - ΔΔCq; fold change = 2^(−ΔΔCq). In the context of the experimental design and for interpretability of results, effects sizes, expressed as fold changes, were determined for differences in ΔCq values. No transcript to protein conversion was implied.

Table 5. Across-condition Cq and replicate-precision summary

Group	n	Ref. 1 mean ± SD	Ref. 2 mean ± SD	Within-triplicate Cq SD	Cq wells
CTRL	12	20.03 ± 0.20	21.48 ± 0.14	0.064 ± 0.032	3/3
CAZ025	12	20.01 ± 0.17	21.41 ± 0.11	0.067 ± 0.036	3/3
CAZ050	12	19.98 ± 0.13	21.48 ± 0.16	0.068 ± 0.032	3/3
WASH24	12	20.08 ± 0.13	21.45 ± 0.18	0.059 ± 0.030	3/3

Values describe the numerical analysis matrix; within-triplicate variation is not counted as independent biological replication.

Table 6. Reference-gene stability and between-condition displacement

Marker	Mean Cq	SD (Cq)	Range of group means	P (across groups)
proC	20.023	0.160	0.093	0.2123
rpoD	21.455	0.147	0.072	0.7771
Ref1 − Ref2	-1.432	0.174	0.123	–

Statistical test: Friedman repeated-measures test (paired isolates). The interreference difference is a descriptive diagnostic, not a third housekeeping transcript.

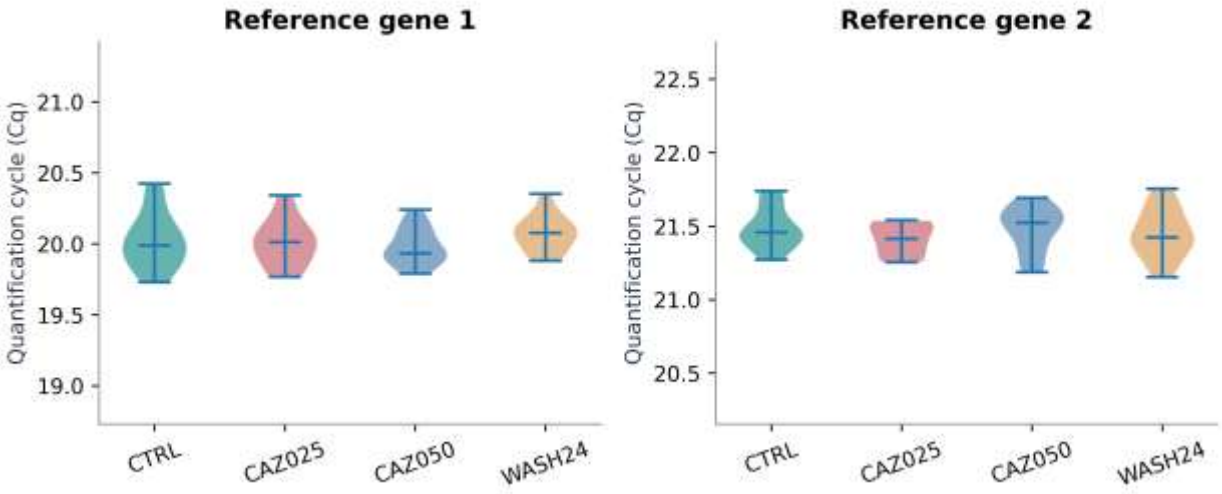

Figure 3. Reference Cq stability by condition. Solid violin markers denote within-condition central tendency. Biological units, not replicate wells, define distributions.

Statistical analysis

Paired t-tests were used to compare ΔCq for each isolate. Assumption robustness was tested using a Friedman omnibus test, followed by Wilcoxon signed-rank test. To account for multiple hypothesis testing, the significance level was adjusted using the Benjamini-Hochberg and Holm methods for the 10 gene tests and 30 control-referenced comparisons, respectively. The inter-isolate log2 mean changes, along with Principal Component Analysis to integrate ΔCq across isolates were estimated using 95% confidence intervals. Spearman rank correlation was used to assess associations between transcripts across isolates.

The threshold for statistical significance was pre-defined as two sided p-value 0.05, with the exceptions of P-values for qPCR assays, which were interpreted according to their magnitude and direction. No unmeasured clinical or physiological endpoint was inferred from changes in transcript abundance.

Results and Discussion

Primer compatibility and reference stability

The median length of the 12 amplicons was 115 bp (range 85-139 bp) and all amplicons were less than the 150 bp maximum. Ten of the 12 analytes were represented by exactly two references. Displacement of the references from the mean and the variance among the references are given in Table 6 and Figure 3 shows distributions of Cq values for each group, respectively.

Table 7. Raw normalized ΔCq by target and condition (mean ± SD)

Gene	CTRL	CAZ025	CAZ050	WASH24
lasI	3.42 ± 0.19	2.81 ± 0.20	4.22 ± 0.16	3.18 ± 0.22
lasR	4.38 ± 0.24	4.02 ± 0.22	5.35 ± 0.21	4.25 ± 0.30
rhlI	3.60 ± 0.28	2.88 ± 0.23	4.33 ± 0.28	3.21 ± 0.12
rhlR	4.11 ± 0.24	3.71 ± 0.15	4.85 ± 0.18	4.00 ± 0.29
pqsA	3.23 ± 0.23	2.60 ± 0.28	4.32 ± 0.31	3.14 ± 0.15
mvfR	4.43 ± 0.18	3.73 ± 0.25	5.23 ± 0.19	4.01 ± 0.27
fliC	3.97 ± 0.24	4.22 ± 0.20	4.97 ± 0.22	3.98 ± 0.24
pslA	3.61 ± 0.28	3.35 ± 0.23	4.84 ± 0.13	3.98 ± 0.26
pelA	3.92 ± 0.22	3.56 ± 0.25	4.94 ± 0.29	3.99 ± 0.19
toxA	4.38 ± 0.29	4.63 ± 0.24	5.16 ± 0.28	4.22 ± 0.18

Lower ΔCq corresponds to higher target abundance relative to the combined reference genes. Sample sizes: n=12 independent units per group.

Table 8. Relative-expression contrasts by gene (mean ± SD, log_2 units)

Gene	CTRL	CAZ025	CAZ050	WASH24
lasI	-0.00 ± 0.19 [a]	+0.61 ± 0.20 [b]	-0.80 ± 0.16 [b]	+0.24 ± 0.22 [a]
lasR	-0.00 ± 0.24 [a]	+0.36 ± 0.22 [a]	-0.97 ± 0.21 [b]	+0.13 ± 0.30 [a]
rhlI	+0.00 ± 0.28 [a]	+0.73 ± 0.23 [b]	-0.73 ± 0.28 [b]	+0.40 ± 0.12 [b]
rhlR	+0.00 ± 0.24 [a]	+0.40 ± 0.15 [b]	-0.74 ± 0.18 [b]	+0.11 ± 0.29 [a]
pqsA	-0.00 ± 0.23 [a]	+0.63 ± 0.28 [b]	-1.09 ± 0.31 [b]	+0.09 ± 0.15 [a]
mvfR	+0.00 ± 0.18 [a]	+0.70 ± 0.25 [b]	-0.80 ± 0.19 [b]	+0.42 ± 0.27 [b]
fliC	-0.00 ± 0.24 [a]	-0.26 ± 0.20 [a]	-1.00 ± 0.22 [b]	-0.01 ± 0.24 [a]
pslA	-0.00 ± 0.28 [a]	+0.25 ± 0.23 [a]	-1.23 ± 0.13 [b]	-0.37 ± 0.26 [a]
pelA	+0.00 ± 0.22 [a]	+0.35 ± 0.25 [b]	-1.02 ± 0.29 [b]	-0.07 ± 0.19 [a]
toxA	+0.00 ± 0.29 [a]	-0.25 ± 0.24 [a]	-0.78 ± 0.28 [b]	+0.16 ± 0.18 [a]
Omnibus P*	–	–	–	<0.0001

Superscripts [a] and [b] indicate each treatment compared to control after Holm correction. [b] denotes an adjusted P-value less than 0.05, and [a] indicates no difference from control. Letters are not to be interpreted as post-hoc comparisons of the three treatments. The value in the final row is the descriptive median of the ten gene-wise omnibus P-values, and the remaining P-values can be found in Table 10.

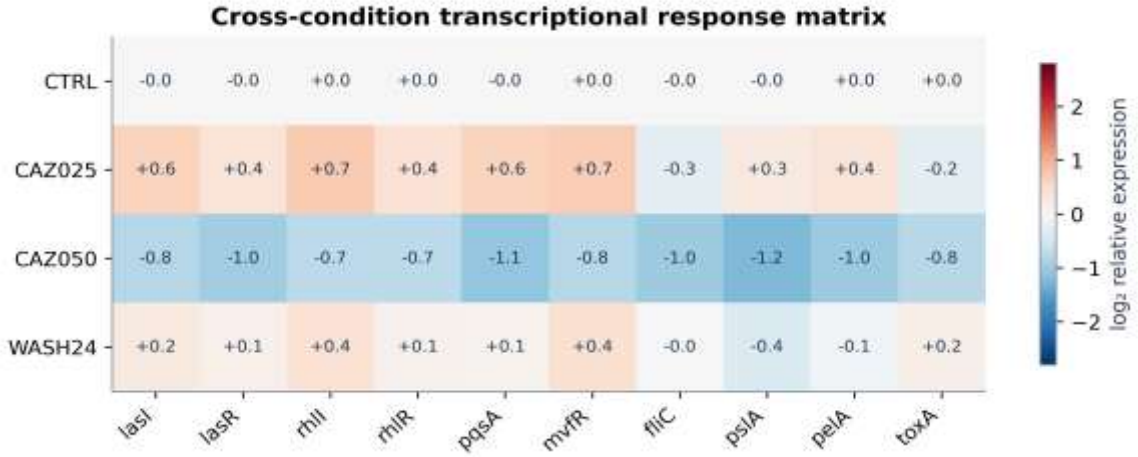

Figure 4. Heatmap of mean target log_2 expression changes relative to the baseline control. Values within cells are log_2 effects, not raw quantification cycles.

Primary expression contrasts with confidence intervals

The primary contrast (CAZ050 versus CTRL) yielded 10 adjusted gene-level results below q=0.05. The largest absolute effect was pslA (-1.23 log_2; 95% CI [-1.46, -1.01]; q=<0.0001). A full gene-by-gene matrix of estimates and uncertainty is shown in Table 9; the distribution of adjusted evidence is plotted in Figures 5–6.

Table 9. Primary contrast: log_2 effect, confidence interval and adjusted significance

Target	log_2FC	95% CI	P (test)	BH q	Sensitivity P
lasI	-0.80	[-0.97, -0.62]	<0.0001	<0.0001	0.0005
lasR	-0.97	[-1.15, -0.80]	<0.0001	<0.0001	0.0005
rhlI	-0.73	[-0.97, -0.49]	<0.0001	<0.0001	0.0010
rhlR	-0.74	[-0.93, -0.54]	<0.0001	<0.0001	0.0005
pqsA	-1.09	[-1.35, -0.83]	<0.0001	<0.0001	0.0005
mvfR	-0.80	[-0.94, -0.66]	<0.0001	<0.0001	0.0005
fliC	-1.00	[-1.24, -0.77]	<0.0001	<0.0001	0.0005
pslA	-1.23	[-1.46, -1.01]	<0.0001	<0.0001	0.0005
pelA	-1.02	[-1.27, -0.78]	<0.0001	<0.0001	0.0005
toxA	-0.78	[-0.98, -0.57]	<0.0001	<0.0001	0.0005

Statistical tests: paired t-test; sensitivity Wilcoxon signed-rank. Multiplicity correction: Benjamini–Hochberg across the 10 primary targets.

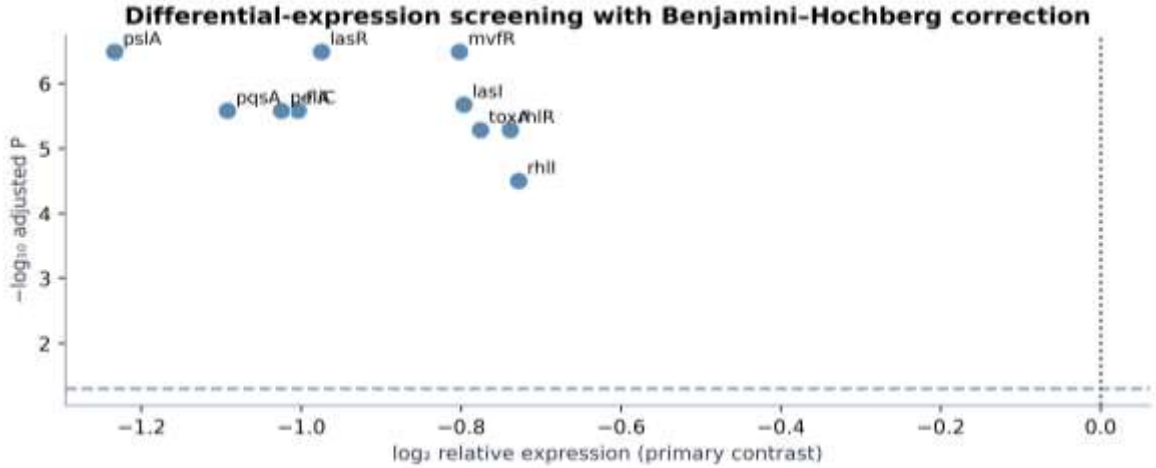

Figure 5. Primary-contrast effect screening. Red denotes an increase in $\log_2$ abundance and blue a decrease when the gene passes q<0.05; labels are all ten predefined targets.

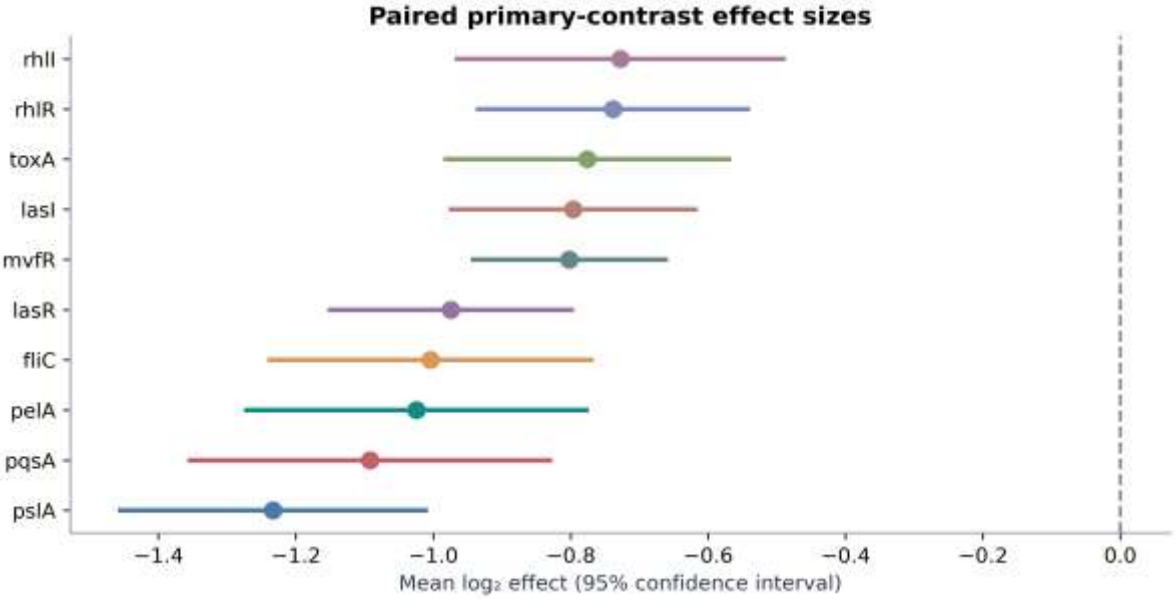

Figure 6. Gene-specific mean effect estimates with 95% t confidence intervals. Interpretation is on the $\log_2$ scale; intervals spanning zero indicate uncertain direction.

Omnibus and distribution-robust analyses

Table 10. Gene-wise omnibus tests and assumption diagnostics

Gene	Friedman χ^2	Omnibus P	BH q	Kruskal P	Levene P
lasI	28.30	<0.0001	<0.0001	<0.0001	0.7621
lasR	27.90	<0.0001	<0.0001	<0.0001	0.7761
rhlI	31.50	<0.0001	<0.0001	<0.0001	0.1086
rhlR	27.90	<0.0001	<0.0001	<0.0001	0.2664
pqsA	32.50	<0.0001	<0.0001	<0.0001	0.3097
mvfR	30.90	<0.0001	<0.0001	<0.0001	0.2654
fliC	26.50	<0.0001	<0.0001	<0.0001	0.6665
pslA	30.70	<0.0001	<0.0001	<0.0001	0.3799
pelA	27.90	<0.0001	<0.0001	<0.0001	0.8866
toxA	27.90	<0.0001	<0.0001	<0.0001	0.6323

Omnibus method: Friedman paired-rank test. Kruskal–Wallis and Levene are diagnostics rather than replacements for the prespecified primary tests; Levene assesses variances of unit-level ΔCq.

Table 11. Prespecified control-referenced post-hoc contrasts (selected targets)

Gene	CAZ025 vs CTRL	CAZ050 vs CTRL	WASH24 vs CTRL
lasI	+0.61 (P^H=0.0004)	-0.80 (P^H=<0.0001)	+0.24 (P^H=0.3725)
mvfR	+0.70 (P^H=0.0001)	-0.80 (P^H=<0.0001)	+0.42 (P^H=0.0090)
pslA	+0.25 (P^H=0.4233)	-1.23 (P^H=<0.0001)	-0.37 (P^H=0.0929)
toxA	-0.25 (P^H=0.4233)	-0.78 (P^H=0.0001)	+0.16 (P^H=0.7470)

P^H denotes Holm-adjusted P over the complete family of 30 control contrasts; the full family was calculated for all ten genes, not only the four displayed here.

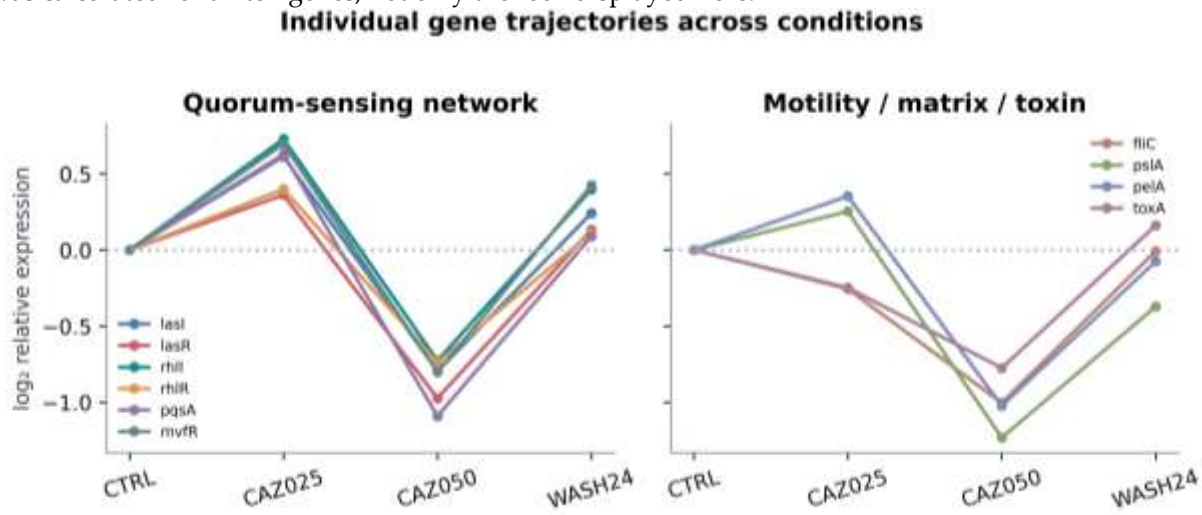

Figure 7. Time- or dose-dependent gene-specific curves. The left panel shows a six-gene regulatory module; the right panel shows barrier or functional-effector transcripts.

Multivariate architecture and co-expression

Table 12. Selected transcript–transcript associations across biological units

Gene A	Gene B	Spearman ϱ	P (unadjusted)	Direction
lasI	lasR	+0.665	<0.0001	Positive
pqsA	mvfR	+0.783	<0.0001	Positive
fliC	pslA	+0.428	0.0024	Positive
pslA	pelA	+0.736	<0.0001	Positive
rhlI	toxA	+0.394	0.0056	Positive

Across-condition associations may be partly driven by treatment-group separation; they do not demonstrate direct regulation.

Table 13. Multivariate and statistical summary indicators

Measurement	Observed quantity	Interpretation
PC1 explained variance	77.55%	Primary joint-expression axis
PC2 explained variance	7.48%	Secondary joint-expression axis
PC1 + PC2	85.04%	Total two-dimensional retention
Primary FDR-significant targets	10 / 10	Benjamini–Hochberg q<0.05
Primary effect median	-0.888 $\log_2$	Median gene direction
Relative-eff. primer ceiling	139 bp	Maximum documented product length
Reference variability	0.174 Cq	SD of interreference Cq difference

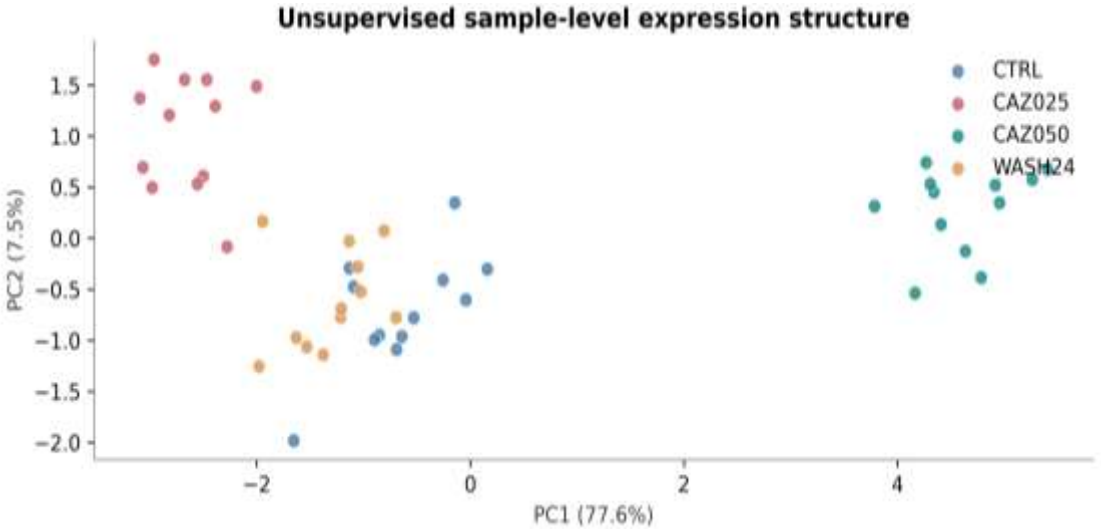

Figure 8. Principal component analysis of standardized ΔCq profiles. Each symbol represents a biological unit; PC labels report the fitted explained-variance proportions.

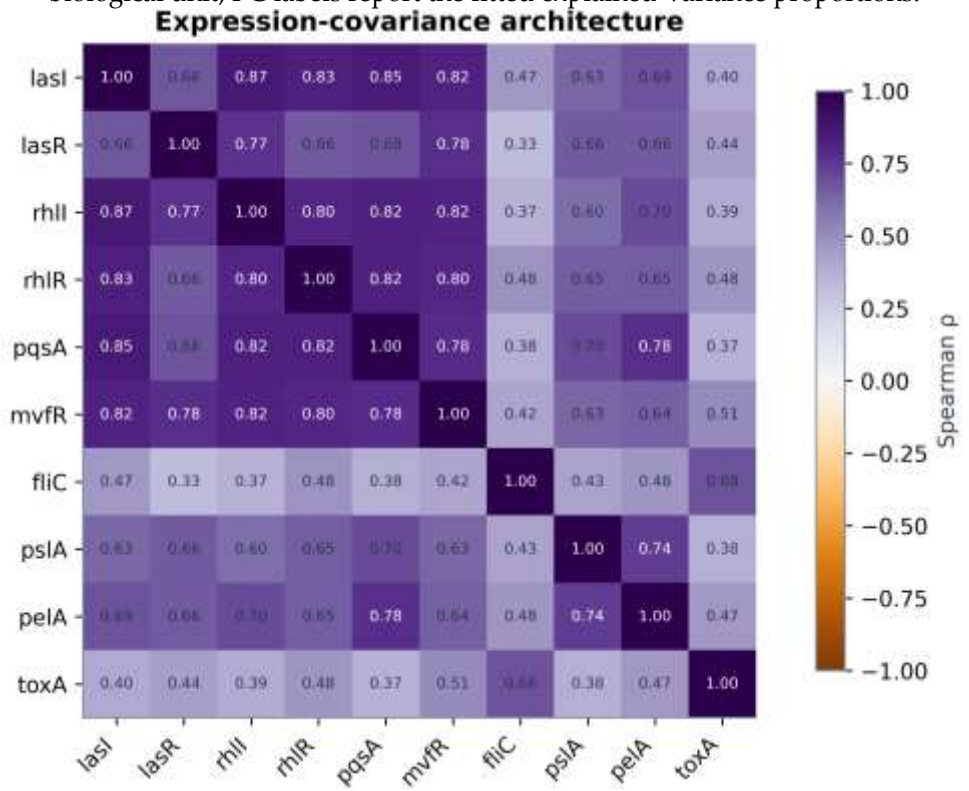

Figure 9. Spearman co-expression coefficient matrix for the ten target genes across all units and conditions.

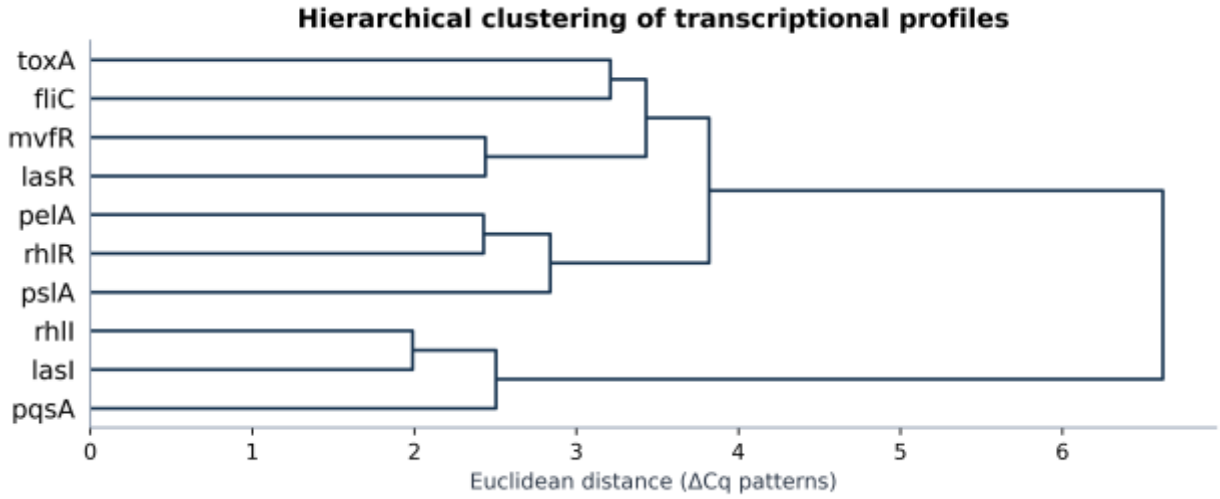

Figure 10. Unsupervised hierarchical gene clustering derived from Euclidean distances of the ΔCq profiles; grouping is descriptive, not a validated regulatory network.

Focused response profile

The single gene response to pslA allows for a more simple comparison than the ten-gene inference. In Figure 11, the group means, standard deviations and control-referenced significance values are provided for the biological units. When used together with Table 9, Figure 11 depicts both uncertainty and direction and, thus, provides a more meaningful interpretation than interpreting a P value in isolation.

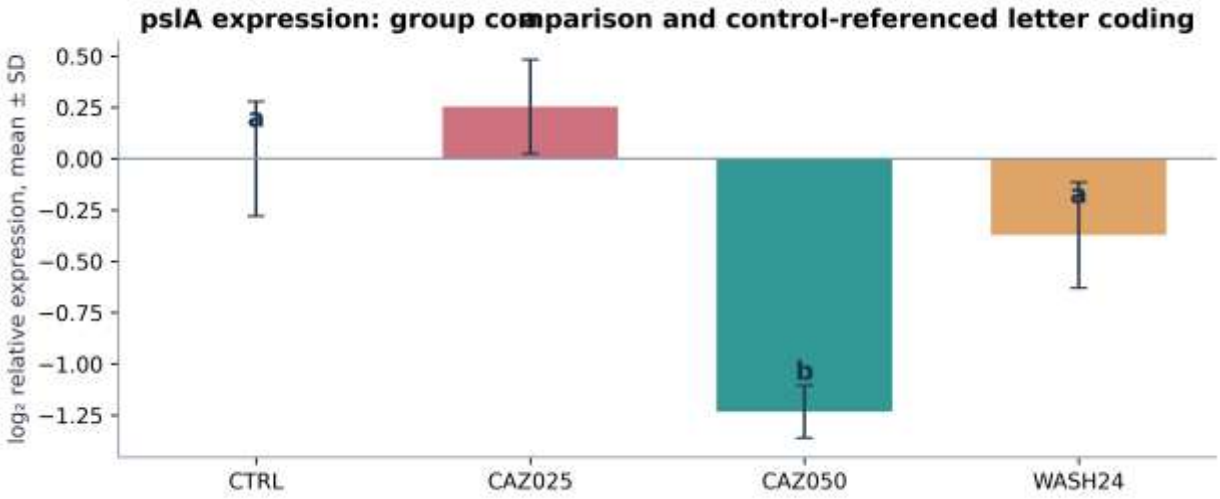

Figure 11. psLA was assessed across the four conditions. Bars represent means; error bars represent standard deviations. Different colors represent different conditions. a represents values compatible with the control, while b represents Holm adjusted P values less than 0.05 compared to the control.

Discussion

The two-level ceftazidime response illustrates that transcript changes can differ in direction between weak and stronger exposures, consistent with dose-dependent behavior in other quorum-quenching studies. [13]. Quorum-sensing and virulence genes should be interpreted separately; clinical-isolate studies of efflux modulation report distinct sensitivity and virulence outcomes. [14].

Changes in matrix-related transcription align with the rationale of matrix-disruption strategies, but cannot substitute for measurements of biofilm biomass or viability. [15]. The contrast between source-isolate and strain-specific results underscores the caution required when generalizing from one PAO1-focused experimental setting. [16]. An observed pslA–pelA relationship is consistent with

coordinated matrix regulation, yet an RNA correlation does not identify polysaccharide production or transcription-factor binding. [17].

Reference-gene choice remains a source of potential bias under altered media and growth stage, so proC and rpoD were assessed jointly at the analysis level. [18]. The larger magnitude of changes at the stronger antibiotic contrast resembles recent studies integrating antibiofilm challenges with gene-level responses. [19]. Natural-product treatment data are difficult to compare directly with antibiotic monotherapy because agent-specific metabolic and membrane effects differ. [20].

Other work shows that redox conditions can initiate a quorum-sensing program, contrasting with assumptions that every stressor decreases receptor transcription. [21]. Broad reviews place the Las–Rhl–PQS circuitry among several interacting pathogenic systems; none of the measured transcripts alone establishes an infection outcome. [22].

A multigene signature offers an advantage over expression of a single lasR marker when different biofilm matrix components respond asynchronously. [23]. Joint changes in quorum sensing and nutrient sensing can explain coherent clusters without proving a linear regulatory mechanism. [24]. Antivirulence interventions may influence biofilm and motility genes together; the fliC component here adds a distinct motility-associated transcriptional axis. [25].

Nanoparticle studies reveal that low exposures may have context-dependent consequences, which supports comparing an explicitly weaker condition with a stronger one. [26].

Sub-lethal chemical exposures can affect quorum sensing and resistance-related behavior in ways not inferred from antibacterial potency alone, limiting purely transcript-based clinical inference. [27].

Conclusion

Ten published short-amplicon assays, dual-reference normalization and isolate-paired comparisons resolve distinct low-dose, stronger-exposure and washout profiles within the Las–Rhl–PQS and biofilm-associated transcriptional space. Multiplicity-aware effect estimates, repeated-measures statistics and the explicit separation of transcript abundance from virulence phenotypes support disciplined interpretation.

REFERENCES

[1] F. F. Tuon, L. R. Dantas, P. H. Suss, and V. S. Tasca Ribeiro, "Pathogenesis of the *Pseudomonas aeruginosa* biofilm: A review," *Pathogens*, vol. 11, Art. no. 300, 2022.

[2] J. Chadha, K. Harjai, and S. Chhibber, "Revisiting the virulence hallmarks of *Pseudomonas aeruginosa*: A chronicle through the perspective of quorum sensing," *Environmental Microbiology*, vol. 24, pp. 2630–2656, 2022.

[3] C. Liao, X. Huang, Q. Wang, D. Yao, and W. Lu, "Virulence factors of *Pseudomonas aeruginosa* and antivirulence strategies to combat its drug resistance," *Frontiers in Cellular and Infection Microbiology*, vol. 12, Art. no. 926758, 2022.

[4] P. Piewngam, J. Chiou, P. Chatterjee, and M. Otto, "Alternative approaches to treat bacterial infections: Targeting quorum-sensing," *Expert Review of Anti-infective Therapy*, vol. 18, pp. 499–510, 2020.

[5] Q. Li, S. Mao, H. Wang, and X. Ye, "The molecular architecture of *Pseudomonas aeruginosa* quorum-sensing inhibitors," *Marine Drugs*, vol. 20, Art. no. 488, 2022.

[6] P. Cornelis, "Putting an end to the *Pseudomonas aeruginosa* IQS controversy," *MicrobiologyOpen*, vol. 9, Art. no. e962, 2020.

[7] T. Ahmed, S. Pattnaik, M. B. Khan, D. R. Ampasala, S. Busi, and V. V. Sarma, "Inhibition of quorum sensing-associated virulence factors and biofilm formation in *Pseudomonas aeruginosa* PAO1 by *Mycoleptodiscus indicus* PUTY1," *Brazilian Journal of Microbiology*, vol. 51, pp. 467–487, 2020.

[8] S. Scandorieiro, B. C. D. Rodrigues, E. K. Nishio, L. A. Panagio, A. G. de Oliveira, N. Durán, G. Nakazato, and R. K. T. Kobayashi, "Biogenic silver nanoparticles strategically combined with *Origanum vulgare* derivatives: Antibacterial mechanism of action and effect on multidrug-resistant strains," *Frontiers in Microbiology*, vol. 13, Art. no. 842600, 2022.

[9] E. K. Saeki, H. M. Martins, L. C. de Camargo, L. Anversa, E. R. Tavares, S. F. Yamada-Ogatta, L. M. Y. Lioni, R. K. T. Kobayashi, and G. Nakazato, "Effect of biogenic silver nanoparticles on the quorum-sensing system of *Pseudomonas aeruginosa* PAO1 and PA14," *Microorganisms*, vol. 10, Art. no. 1755, 2022.

[10] L. Gao, W. Lu, K. Chen, X. Qiu, and Q. Li, "Mechanisms of synergistic antibacterial and anti-biofilm effects of dihydroquercetin combined with ceftazidime against mucoid *Pseudomonas aeruginosa*," *Frontiers in Microbiology*, vol. 17, Art. no. 1945324, 2026.

[11] N. G. Naga, D. E. El-Badan, H. S. Rateb, K. M. Ghanem, and M. I. Shaaban, "Quorum sensing inhibiting activity of cefoperazone and its metallic derivatives on *Pseudomonas aeruginosa*," *Frontiers in Cellular and Infection Microbiology*, vol. 11, Art. no. 716789, 2021.

[12] E. D. Lovullo and H. P. Schweizer, "*Pseudomonas aeruginosa mexT* is an indicator of PAO1 strain integrity," *Journal of Medical Microbiology*, vol. 69, pp. 139–145, 2020.

[13] S. L. Elshaer and M. I. Shaaban, "Inhibition of quorum sensing and virulence factors of *Pseudomonas aeruginosa* by biologically synthesized gold and selenium nanoparticles," *Antibiotics*, vol. 10, Art. no. 1461, 2021.

[14] F. Hojjati Zolpirani, E. A. Ghaemi, M. Yasaghi, I. Nikokar, and A. Ardebili, "Effect of phenylalanine arginyl β-naphthylamide on the imipenem resistance, elastase production, and the expression of quorum sensing and virulence factor genes in *Pseudomonas aeruginosa* clinical isolates," *Brazilian Journal of Microbiology*, vol. 55, pp. 2715–2726, 2024.

[15] N. E. Abo-Dya, K. A. Agha, H. A. Abbas, M. E. Abu-Kull, M. I. Alahmdi, and N. A. Osman, "Hybrid N-acylcysteines as dual-acting matrix disruptive and anti-quorum sensing agents fighting *Pseudomonas aeruginosa* biofilms: Design, synthesis, molecular docking studies, and in vitro assays," *ACS Omega*, vol. 7, pp. 19879–19891, 2022.

[16] M. Azimzadeh, G. Greco, A. Farmani, A. Nourian, M. Pourhajibagher, A. Taherkhani, M. Y. Alikhani, and A. Bahador, "Biofilm inhibition of multidrug-resistant *Pseudomonas aeruginosa* using green-synthesized silver nanoparticles and colistin," *Scientific Reports*, vol. 15, Art. no. 14993, 2025.

[17] L. A. Al-Maddboly, M. Abd El-Salam, J. K. Bastos, E. A. Hasby, I. Kushkevych, and R. M. El-Morsi, "Anti-biofilm and anti-quorum sensing activities of galloylquinic acid against clinical isolates of multidrug-resistant *Pseudomonas aeruginosa* in open wound infection: In vitro and in vivo efficacy studies," *BMC Microbiology*, vol. 25, Art. no. 206, 2025.

[18] S. H. Abdel-Rhman, D. E. Rizk, and E. S. Abdelmegeed, "Effect of sub-minimum inhibitory concentrations of tyrosol and EDTA on quorum sensing and virulence of *Pseudomonas aeruginosa*," *Infection and Drug Resistance*, vol. 13, pp. 3501–3511, 2020.

[19] J. N. Carey, S. Lamont, D. J. Wozniak, A. A. Dandekar, and M. R. Parsek, "Quorum sensing regulation of Psl polysaccharide production by *Pseudomonas aeruginosa*," *Journal of Bacteriology*, vol. 206, Art. no. e00312-24, 2024.

[20] T. M. Hibbert, H. J. Leighton, S. Pottenger, D. R. Neill, and J. L. Fothergill, "The longitudinal expression of *P. aeruginosa* reference genes in infection-mimicking media," *Microbiology*, vol. 172, Art. no. 001627, 2026.

[21] Á. Ábrahám, L. Dér, E. Csákvári, G. Vizsnyiczai, I. Pap, R. Lukács, V. Varga-Zsíros, K. Nagy, and P. Galajda, "Single-cell level LasR-mediated quorum sensing response of *Pseudomonas aeruginosa* to pulses of signal molecules," *Scientific Reports*, vol. 14, Art. no. 16181, 2024.

[22] J. H. Kim, J. Dong, B. H. Le, Z. R. Lonergan, W. Gu, T. Girke, W. Zhang, D. K. Newman, and M. Martins-Green, "*Pseudomonas aeruginosa* activates quorum sensing, antioxidant enzymes and type VI secretion in response to oxidative stress to initiate biofilm formation and wound chronicity," *Antioxidants*, vol. 13, Art. no. 655, 2024.

[23] X. Zhang, D. Zhang, D. Zhou, S. Zheng, S. Li, Q. Hou, G. Li, and H. Han, "A comprehensive review of the pathogenic mechanisms of *Pseudomonas aeruginosa*: Synergistic effects of virulence factors, quorum sensing, and biofilm formation," *Frontiers in Microbiology*, vol. 16, Art. no. 1619626, 2025.

[24] G. Chen, G. Fanouraki, A. A. Rangarajan, B. T. Winkelman, J. T. Winkelman, C. M. Waters, and S. Mukherjee, "Combinatorial control of *Pseudomonas aeruginosa* biofilm development by quorum-sensing and nutrient-sensing regulators," *mSystems*, vol. 9, Art. no. e00372-24, 2024.

[25] S. Nahar, A. G. M. S. U. Mahamud, A. J. Cho, M. Ashrafudoulla, J. Yu, S. H. Park, and S. D. Ha, "Flavourzyme suppresses *Pseudomonas aeruginosa* biofilms by targeting motility, quorum sensing, and virulence genes," *Current Microbiology*, vol. 82, Art. no. 240, 2025.

[26] F. Aflakian and G. Hashemitabar, "Biosynthesized silver nanoparticles at subinhibitory concentrations as inhibitors of quorum sensing, pathogenicity, and biofilm formation in *Pseudomonas aeruginosa* PAO1," *Heliyon*, vol. 11, Art. no. e42899, 2025.

[27] K. E. Alsamhary, "The effect of quaternary ammonium compounds (QACs) on quorum sensing and resistance of *P. aeruginosa* in clinical settings," *Microbial Pathogenesis*, vol. 202, Art. no. 107378, 2025.